Title
Right Ventricular Function and T1-Mapping in Boys With Duchenne Muscular Dystrophy

Journal
Journal of Magnetic Resonance Imaging, 54(5)

ISSN
1053-1807

Authors
Dual, Seraina A
Maforo, Nyasha G
McElhinney, Doff B
et al.

Publication Date
2021-11-01

DOI
10.1002/jmri.27729

Peer reviewed

HHS Public Access

Author manuscript

J Magn Reson Imaging. Author manuscript; available in PMC 2022 November 01.

Published in final edited form as:

J Magn Reson Imaging. 2021 November ; 54(5): 1503–1513. doi:10.1002/jmri.27729.

Right Ventricular Function and T1-mapping in Boys with Duchenne Muscular Dystrophy

Seraina A. Dual, PhD[1,2,6], **Nyasha G. Maforo**[3,4], **Doff B. McElhinney, MD**[2], **Ashley Prosper, MD**[4], **Holden H. Wu, PhD**[3,4], **Shiraz Maskatia, MD**[5,7], **Pierangelo Renella, MD**[4,8], **Nancy Halnon, MD**[9], **Daniel B. Ennis, PhD**[1,6,7]

[1]Department of Radiology, Stanford University, Palo Alto, CA, USA

[2]Department of Cardiothoracic Surgery, Stanford University, Palo Alto, CA, USA

[3]Physics and Biology in Medicine Interdepartmental Program, University of California, Los Angeles, CA, USA

[4]Department of Radiological Sciences, University of California, Los Angeles, CA, USA

[5]Department of Pediatrics, Stanford University, Palo Alto, CA, USA

[6]Cardiovascular Institute, Stanford University, Palo Alto, CA, USA

[7]Maternal & Child Health Research Institute, Palo Alto, CA, USA

[8]Children's hospital Orange County, University of California, Irvine, CA, USA

[9]Department of Medicine (Cardiology), University of California, Los Angeles, CA, USA

Abstract

BACKGROUND: Clinical management of boys with Duchenne muscular dystrophy (DMD) relies on in depth understanding of cardiac involvement, but right ventricular (RV) structural and functional remodeling remains understudied.

PURPOSE: To evaluate several analysis methods and identify the most reliable one to measure RV pre- and post-contrast T1 (RV-T1) and to characterize myocardial remodeling in the RV of boys with DMD.

STUDY TYPE: Prospective.

POPULATION: Boys with DMD (N=27) and age-/sex-matched healthy controls (N=17) from two sites.

FIELD STRENGHT/SEQUENCE: 3.0T using balanced steady state free precession (bSSFP), motion-corrected phase sensitive inversion recovery and modified Look-Locker inversion recovery (MOLLI) sequences.

ASSESSEMENT: Biventricular mass (Mi), end-diastolic volume (EDVi) and ejection fraction (EF) assessment, tricuspid annular excursion (TAE), late gadolinium enhancement (LGE), pre- and

Corresponding author: Seraina Dual, 780 Welch Rd., CA-94304 Palo Alto, +1 702 355 66 02, duals@stanford.edu.

Clinical trial registration: https://clinicaltrials.gov/ct2/show/NCT02834650.

post-contrast myocardial T1 maps. The RV-T1 reliability was assessed by three observers in four different RV regions of interest (ROI) using intra-class correlation (ICC).

STATISTICAL TESTS: The Wilcoxon rank sum test was used to compare RV-T1 differences between DMD boys with negative LGE(–) or positive LGE(+) and healthy controls. Additionally, correlation of pre-contrast RV-T1 with functional measures was performed. A p value <0.05 was considered statistically significant.

RESULTS: A one-pixel thick RV circumferential ROI proved most reliable (ICC>0.91) for assessing RV-T1. Pre-contrast RV-T1 was significantly higher in boys with DMD compared to controls. Both LGE(–) and LGE(+) boys had significantly elevated pre-contrast RV-T1 compared to controls (1543[1489–1597]ms and 1550[1402–1699]ms vs. 1436[1399–1473]ms, respectively). Compared to healthy controls, boys with DMD had preserved RVEF (51.8(9.9)% vs. 54.2(7.2)%, p=0.31) and significantly reduced RVMi (29.8(9.7)g vs. 48.0(15.7)g), RVEDVi (69.8(29.7)mL/m^2 vs. 89.1(21.9)mL/m^2), and TAE(22.0(3.2)cm vs 26.0(4.7)cm). Significant correlations were found between pre-contrast RV-T1 and RVEF (β=–0.48%/ms) and between LV-T1 and LVEF (β=–0.51%/ms).

DATA CONCLUSION: Pre-contrast RV-T1 is elevated in boys with DMD compared to healthy controls and is negatively correlated with RVEF.

Keywords

Duchenne muscular dystrophy; Cardiomyopathy; Cardiovascular magnetic resonance; Late gadolinium enhancement; Myocardial remodeling; T1-mapping

INTRODUCTION

Duchenne muscular dystrophy (DMD) is an X-linked genetic muscular disorder that develops in 1 out of 5,000 boys(1, 2) and causes progressive muscle damage. Boys with DMD first exhibit skeletal muscle weakness. This is followed by respiratory dysfunction and progressive decline in heart function by early adulthood(3), which are the leading causes of death in DMD.(4, 5) Currently, the impact of respiratory insufficiency on right ventricle (RV) function remains incompletely understood, but may accelerate the rate of cardiac disease progression in DMD.(4–6) Hence, imaging-based detection of changes in RV structure and function may allow for the timely initiation of respiratory support, as well as cardioprotective and perhaps more advanced gene therapies.(3)

Magnetic resonance imaging (MRI) is an established tool in the clinical management of DMD.(7) MRI allows for the detection of both functional and tissue microstructure changes in this high-risk patient cohort,(3) providing reliable measures of RV and left ventricular (LV) volumes, mass, strain, and ejection fraction (EF). Late gadolinium enhancement (LGE) MRI reveals changes in tissue microstructure, such as the presence of DMD-associated focal fibrosis in the sub-epicardium.(8, 9) The presence of LGE is the current reference standard to monitor tissue remodeling in DMD, but it cannot detect diffuse disease patterns and the qualitative assessment of LGE is operator dependent.(10) Diffuse disease is better studied using myocardial pre-contrast T1 mapping, which is a quantitative, non-invasive method for the evaluation of diffuse microstructural remodeling in boys with DMD.(11–13)

Furthermore, the combination of pre- and post-contrast T1 mapping allows estimation of the extracellular volume (ECV) fraction.(11, 14, 15)

Currently, CMR imaging in DMD focuses on the LV. However, ongoing efforts to understand cardiac involvement in DMD focus on the propensity to develop biventricular failure.(4, 6) In a retrospective DMD patient cohort (n=272), a significant moderate correlation (r=0.62) was found between RV and LV EF; however, in the seven patients with severe LV dysfunction (LVEF<30%), RVEF was relatively preserved (49.7±12.9%). While the RVEF did decline at later stages, the decline in RV function was not noted during early stages of disease.(16) In addition, the RV fibrosis has not been well-studied in DMD patients.

Assessment of RV fibrosis in the pediatric population is difficult owing to the thin-wall and high trabeculation, which makes the analysis more technically challenging and time consuming. T1 mapping offers a quantitative analysis approach that has demonstrated an elevated T1 value in the LV even during early stages of DMD.(13) Reports in the RV of boys with DMD, however, are lacking. Hence, methods to reliably evaluate pre-contrast RV-T1 as well as RV-ECV are needed to quantify myocardial remodeling in DMD.

Therefore, the aims of this study were: (1) to evaluate several methods and to identify a reliable methodology to assess RV-T1 and RV-ECV; and (2) to compare RV-T1 and RV-ECV, presence of LGE, increased ventricular volumes, and decreased EFs as methods of assessing cardiac disease progression in boys with DMD.

MATERIALS AND METHODS

Ethics and study population

Boys with DMD (N=27) and age-matched healthy controls (N=17) were prospectively enrolled for this study at 3T (Skyra, Siemens Healthcare, Erlangen, Germany). One additional boy with DMD was enrolled but could not complete the T1 mapping of the exam, due to patient discomfort. The multi-center study was approved by the IRB and parental written consent and subject assent were obtained. Boys with DMD were recruited from neuromuscular clinics at two children’s hospitals and healthy controls from the community. On the day of the MRI exam, all boys with DMD were administered a hematocrit test for the calculation of subject specific ECV.

MRI exam

All detailed acquisition parameters are summarized in Table 1.

Cardiac function

The exam included standard functional imaging using a free-breathing retrospectively binned balanced steady state free precession (bSSFP) cine sequence.(17) All cine imaging spanned the entire heart from base to apex using short-axis slices. Vertical and horizontal long axis (VLA, HLA) views were also acquired.

T1 mapping

Two pre-contrast and post-contrast myocardial T1 maps (Scan-1 and Scan-2) were acquired in separate breath holds during diastasis for a single mid-ventricular short-axis slice with a motion-corrected (MOCO) modified Look-Look inversion recovery (MOLLI) sequence, (18) as described previously.(13) Contrast (Gd-BOPTA, MultiHance, Bracco Diagnostics) was administered (0.1mmol/kg) only to boys with DMD, followed by LGE imaging and post-contrast T1 mapping (at 18±6.1 min).

LGE—LGE imaging was acquired using a free-breathing motion corrected phase sensitive inversion recovery (PSIR) sequence (19) in the short-axis view spanning base to apex.

Image Analysis

Functional Evaluation: Three clinicians (**, **, and **, with 12, 8, 8, years of experience) performed RV and LV volumetry (Circle, Cardiovascular Imaging Inc. or Medis, Cardiovascular Imaging) using the short-axis cine images. Measured parameters included: LVEF, RVEF, LV and RV end-systolic and end-diastolic volumes (LVESVi, LVEDVi) and LV and RV mass (LVMi, RVMi), indexed by body surface area (BSA). Trabeculations were included in the measurement of chamber volume and excluded from the RV mass. The thresholds used to distinguish normal from decreased systolic function were: LVEF≥55% and RVEF≥50%.(20) Additionally, the tricuspid annular excursion (TAE) was used to manually measure RV longitudinal motion (total systolic displacement the right atrioventricular groove in the HLA view) (21). HLA cines were not available in all boys, so TAE was only available in 19/27 DMD and 10/17 healthy controls.

LGE Evaluation: The presence or absence of LGE was assessed by ** and ** according to the AHA 17-segment model, where the presence of LGE in one segment was noted as LGE(+) and absence of any LGE was considered LGE(–).

Pre-contrast T1 Evaluation: Grey-scale pre-contrast T1 maps were generated according to Maforo et al. 2020(13) and used to define the regions of interest (ROI) (see Figure 1). In order to establish the most reliable method to measure T1 in the RV, we evaluated four ROIs: one pixel (1px = 1.9 mm) and three pixel (3px = 5.7 mm) thick ROIs along the RV circumference, a segment within the RV lateral wall, and a segment within the RV inferior wall. All RV ROIs were delineated, avoiding blood pool and epicardial fat. The 3px circumferential ROI was dilated based on the delineation of the 1px ROI and might include surrounding blood or fat. Blood pool T1 measurements were obtained for the RV and LV, excluding papillary muscles and trabeculations.

Relative Pre-contrast T1: T1 from one ROI in a segment of the LV lateral wall and another ROI in a segment of the septal wall provided an intra-subject reference. We then computed the RV-T1 difference with respect to the interventricular septum (ΔRV_{Sep}), the LV (ΔRV_{LV}), as well as between the LV and the septum (ΔLV_{Sep}).

Extracellular volume fraction: Image registration was done (15) and with knowledge of patient's hematocrit pixelwise ECV calculated.(13)

Quality Assessment of RV-T1: In order to establish a reliable method of RV-T1 mapping, we compared all four RV ROIs. ROIs were drawn repeatedly for all subjects by one researcher (O1a=**, O1b=**) and two clinicians (O2=**, O3=**). Furthermore, the definition of the region of interests was repeated for both scans (Scan-1, Scan-2) by the first observer. The observers included all images in the analysis for which the bounds of the RV myocardium were distinguishable from surrounding tissue. The feasibility of analysis was calculated as percentage of included images from the total number of available images.

The criteria for a reliable ROI ordered by priority were: (A) high intra-scan, intra- and inter-observer intra-class correlation coefficient (ICC > 0.90); (B) an acceptable number of pixels (>20 pixels);(14, 22) (C) coefficient of variation (COV < 10% across all pixels in ROI) (23); and (D) a feasibility of analysis above 75%. The criteria were applied to the healthy cohort and consequently the most reliable ROI was used in further analyses. Repeatability was reported for both groups.

Statistical analysis

The subjects were divided into the three groups: boys with DMD that were LGE(+) or LGE(–), and healthy controls. Demographic, inter-center, and functional differences were assessed using the Wilcoxon rank-sum test. Values were reported as median (interquartile range) accounting for the small number of patients. Summary statistics of T1 and ECV for each ROI were extracted as mean ± standard deviation values. A p-value < 0.05 was considered significant.

Quality assessment of RV-T1—For both groups, intra-class correlation coefficients (ICC) were reported for intra-scan repeatability (Scan-1, Scan-2) and for the intra-observer agreement (O1a, O1b). Additionally, we reported the bias (μ) and the limits of agreement (LOA) of the Bland-Altman method.(24) Agreement among readers (O1, O2, O3) was assessed by ICC from a mixed-effects model with the reader as a fixed effect and the subject as a random effect.

Group-wise comparison—For comparisons of repeated measurements of T1 values between groups, mean measurement per group and 95% confidence intervals were estimated and adjusted for clustering within subject. Univariate comparisons of pre-contrast T1 measurements between groups were made with a Wilcoxon rank-sum test adjusted for clustering. Prediction of DMD status (control vs. LGE(–), and control vs. LGE(+) using RV-T1 was tested using a logistic regression with RVM and body mass index (BMI) as covariates, adjusted for clustering.

Correlation with established methods—Disease progression in DMD patients was investigated using a correlation analysis of RV-T1 and lateral LV-T1 to predict low LVEF, low RVEF, high LVEDVi, high RVEDVi, and the presence of LGE.

RESULTS

Study population

Compared to healthy controls, boys with DMD had significantly faster heart rates and were shorter, hence they had larger BMI and smaller BSA (Table 2). DMD LGE(+) boys had significantly lower heart rates compared to DMD LGE(–) boys. The LGE(+) boys with high RV-T1, stratified by median, were on average 8[2] years older than the LGE(+) boys with low RV-T1 (see supporting information). Boys recruited across the two centers were not different with respect to prevalence of DMD or LGE, BMI, age, HR, or RVM. None of the boys with DMD required ventilation and three were still ambulatory.

Functional metrics

Standard functional measurements for the LV and RV were compared between subgroups (Table 2). LVEF was significantly reduced in boys with DMD (50.1(11.7)% vs. 57.9(5.8)%, $p < 0.05$) compared to healthy controls, while LVMi (46.1(16.0)g vs. 56.7(29.6)g, $p=0.85$) was preserved. Boys with DMD had preserved RVEF (51.8(9.9)% vs 54.2(7.2)%, $p=0.31$.), but significantly reduced RVMi (29.8(9.7)g vs. 48.0(15.7)g, $p<0.05$) and RVEDVi (69.8(29.7)mL/m^2 vs. 89.1(21.9)mL/m^2, $p<0.05$) compared to healthy controls. Within the DMD group, 29% had normal LVEF and RVEF; 32% had low LVEF, but normal RVEF; 7% had low RVEF and normal LVEF; and 32% had low LVEF and RVEF. Furthermore, boys with DMD also showed significantly lower TAE (22.0(3.2)mm vs. 26.0(4.7)mm, $p<0.05$) compared to healthy controls. DMD LGE(+) boys had significantly higher LVEDVi, higher LVESVi and lower LVEF compared to LGE(–) boys (all $p<0.05$, see Table 2).

Quality assessment of RV-T1

The 1px circumferential ROI was the most reliable to assess RV-T1 values based on values obtained in healthy boys (Figure 2). The number of pixels in the 1px and 3px ROIs was 65px and 196px, respectively, while in the RV lateral and inferior segment ROIs the average number was 23px and 25px (equivalent to 0.72cm^2 in our study). Mean RV-T1 was significantly elevated ($p<0.05$) with respect to LV-T1 in all RV ROIs, except the inferior wall segment. In the lateral wall segment, the coefficient of variation was the smallest (6.0%), but this was at the expense of low inter-observer agreement (ICC=0.60) (see Table 3). In boys with DMD, intra-scan, intra-observer, and inter-observer agreement was highest for the 1px ROI (Table 3, see Table 1 in the supporting information for data in healthy boys). Considering the high reproducibility, we focus on reporting measurements for the circumferential 1px ROI, bearing in mind the elevated coefficient of variation of 13.4% (above suggested 10%) in this ROI.

Pre-contrast RV-T1

Circumferential 1px RV-T1 was 108ms higher in boys with DMD compared to controls ($p<0.05$) (Figure 3A). In the univariate analysis, 1px RV-T1 in LGE(–) boys was significantly higher compared to controls, but not LGE(+) boys ($p=0.19$) (Figure 3B). Accounting for RVM and BMI in the multivariate model, the 1px RV-T1 predicted LGE(+) boys from healthy controls (OR=1.03, 95% CI: 1.01–1.06, $p<0.05$; Table 4). In all boys, the

pre-contrast 1px RV-T1 was significantly higher than pre-contrast LV-T1. LV-T1 in LGE(+) boys compared to healthy controls was significantly elevated in the lateral wall and in the septum (Table 4).

Relative measure of pre-contrast RV-T1

The septal T1 measurement was similar across groups (Figure 3C). ΔRV_{LV}-T1 in LGE(–) boys was significantly different compared to controls (Figure 3D). Univariate comparison revealed no difference comparing ΔRV_{Sep}-T1 across groups. However, the use of ΔRV_{Sep}-T1 to distinguish between LGE(−) boys with DMD and controls by logistic regression was significant (OR=1.02, 95% CI: 1.01–1.04, $p<0.05$; Table 4). Furthermore, for ΔRV_{Sep}-T1 we found a significant difference ($p<0.05$) between the model predicting LGE(–) and LGE(+) from controls. ΔRV_{LV}-T1 was significantly different for LGE(–) and LGE(+) boys compared to controls (both $p<0.05$; Table 4).

Correlation of pre-contrast RV-T1 and disease measures

Circumferential RV-T1 was negatively correlated with RVEF and LV-T1 was negatively correlated with LVEF (Figure 4). Both RV-T1 and LV-T1 were positively correlated with LVEDVi. RV-T1 and LV-T1 were not significantly different ($p=0.12$ and $p=0.57$) in their correlation with RVEF and LVEF respectively. There was a significant difference in LV-T1 between the LGE(–) and LGE(+) group (1335(70) ms vs. 1409(76) ms, $p<0.05$), but not for RV-T1 (1502(78.08) ms vs. 1531(173.8) ms, p-value=0.92). The inter-quartile range of RV-T1 was increased for the LGE(+) compared to all other groups.

Extra-cellular volume fraction

The agreement across scans and observers of RV-ECV was high and comparable to the reliability of pre-contrast RV T1 (see Table 2 in supporting information); interobserver agreement exhibited was >0.90 for both 1px and 3px RV circumferential ROIs. We did not find a significant difference between LGE(–) boys compared to LGE(+) boys in RV-ECV in the 1 px ROI (44.4[39.9 – 48.9]% vs. 41.1[32.0 – 47.2]%, $p=0.9$).

DISCUSSION

The main finding of this study is that pre-contrast RV-T1 is elevated in boys with DMD compared to healthy controls and is negatively correlated with RVEF. Furthermore, the results show that RV-T1 can be measured reliably using a 1-pixel thick line along the circumference of the RV, establishing a novel, reliable methodology for T1-mapping in the RV.

The use of circumferential 1px RV-T1 proved to be a reliable method to measure T1 in the thin wall of the RV in this pediatric study cohort. It resulted in a consistent mean RV-T1, constitutes a good tradeoff between size and COV, and most importantly was reliable across scans, readings, and observers. The current clinical consensus is that measurement of RV-T1 is not recommended, because breath-held parametric techniques are thought to insufficiently resolve the thin RV wall from the blood pool.(22, 25) A study assessing RV post-contrast T1 in adolescents (13.4±2.8 years) found elevated post-contrast T1 values (392±72 ms vs.

333±62 ms, $p<0.05$) in the anterior RV wall of patients with Tetralogy of Fallot compared to healthy controls at 1.5T.(26) he RV-circumferential method has the advantage of including on average three times more pixels, contributing to a more reliable estimate. The results of our study show that RV-T1 is clinically feasible using MRI at 3T if measured along the 1px circumference. Care should be taken when interpreting RV lateral and inferior wall segments because the absence of clear landmarks results in high observer variability. Future work should address variability of the RV-T1 along lateral and inferior parts of the 1px circumference.

The clinical interpretation of T1 mapping values currently requires institutional standards owing to the variability in T1 measurements between scanners and centers.(22) ECV has been suggested as a more reliable marker of diffuse fibrosis owing to less dependence on the specific MRI scanner field strength, pulse sequence, and contrast agent kinetics than pre-contrast T1 alone.(11, 14, 15) In our study, RV-ECV did not distinguish boys with DMD and positive LGE vs. negative LGE. LV-ECV has been observed to be elevated for LGE(+) boys relative to LGE(−) boys with DMD,(13)mA suggesting difficulties in registering pre- and post contrast images. Alternatively, a relative measurement of pre-contrast T1 against a stable intra-subject reference may mitigate these concerns. Previous reports suggest that pre-contrast T1 values in the septum may(13) or may not(11) remain stable across healthy boys and boys with DMD. In this study, no difference in septal pre-contrast T1 was found between groups. Furthermore, if measured relative to the septum, RV-T1 becomes the strongest predictor of DMD status, when considering BMI and RVM as covariates. The difference between LV-T1 and RV-T1 was highest in LGE(−) boys and normalized in LGE(+) boys. Our findings support the use of relative measures in boys with DMD, as the septum is relatively spared during cardiac disease progression in DMD.(13)

The values of RV-T1 at 3T were found to be consistent with previous studies and help to establish reference values for the RV in male healthy controls and DMD. A direct comparison with human data at 3T cannot be made, as current studies at 3T which use T1 mapping in the RV do not report pre-contrast T1-values for healthy controls.(27–29) Multiple studies have shown that T1 values measured in the RV have are longer than T1 values measured in the LV for healthy subjects at 1.5T (30) and also in a pulmonary hypertension animal model at 3T.(31) Our study echoes previous findings, as we found higher RV-T1 than LV-T1 in both healthy boys and boys with DMD. The elevated RV-T1, with respect to LV-T1, may be due to the naturally increased collagen content of the RV wall.(32) A previous study healthy controls (33±8y) acquired LV-T1 at 1.5 T and compared it to RV-T1 (956(25) ms and 1016(61) ms) during systole, where the myocardium is thicker. (30) In comparison, a normative study in children (14±3y) has reported slightly higher values for LV-T1 (1008±31ms) at 1.5T. The RV-T1 values in the 1.5T study were about 400 ms lower than the measurements at 3T in our pediatric control cohort (13±4y). The differences may be attributed to the physics governing lower T1 values at 1.5T compared to 3T, (33) scanner variability, and potentially a higher proportion of blood pool in the RV wall measurements of smaller hearts.

We found RV-T1 mapping by CMR to be a reliable and a useful tool for assessing measures associated with diffuse fibrosis. Pre-contrast RV-T1 was elevated in boys with DMD, and

distinguished controls from LGE(–) and LGE(+) boys. Previously, elevated pre-contrast T1 in the LV has been shown to indicate increased levels of diffuse myocardial fibrosis.(11, 34, 35) Furthermore, we have previously shown increased T1 measurements and ECV in the LV in the same cohort, wherein the findings indicated that increased values of T1 precede detectable presence of LGE.(13) In the current study, we found that pre-contrast RV-T1 was increased in boys with DMD, suggestive of increased levels of diffuse fibrosis not only in the LV, but also in the RV. Apart from diffuse fibrosis, the measured T1 values may also be elevated due to edema owing to steroids or tissue injury and resulting inflammation. In summary, functional and structural data obtained in this work supports the notion that heart failure in DMD affects both ventricles.(6, 36)

The clinical implications of the results presented in this study for treatment of boys with DMD are two-fold. First, boys with DMD typically develop respiratory issues prior to heart failure.(1) Pre-clinical studies have informed the hypothesis that respiratory dysfunction and resulting hypoxia will result in constriction of the pulmonary arteries and hence increase afterload seen by the RV.(4) Hence, respiratory support strategies might affect right heart function. Abnormal RV function in DMD in our cohort is evidenced by significantly lower RVM and lower TAE, a measure of RV longitudinal contraction, compared to healthy controls. RVEF was not significantly reduced, which helps highlight how insensitive RVEF may be. Furthermore, we saw large variability of RV-T1 in the LGE(+) group. A potential hypothesis is that therapeutic strategies such as respiratory support or medical treatments may change the degree of diffuse fibrosis in the right heart in older patients. Second, the evaluation of RV function is gaining importance since the increased use of left ventricular assist devices (LVAD) as an end-stage therapy in DMD.(36, 37) RV failure post LVAD-implantation is seen in up to 25% of patients,(38) and poses a risk to the potentially fibrotic RV in DMD. In summary, detection of changes in RV function and structure may allow for adequate initiation of respiratory support, as well as support optimal patient selection for the placement of an LVAD.(3) Correlation of RV-T1 and pulmonary function should be considered for future work.

Limitations

The primary limitations of the study were small cohort size, analysis of only a single mid-ventricular slice and technical factors associated with heart rate and RV assessment plus the cohort size. Significantly faster heart rates were detected in DMD group compared to healthy controls, and LGE(+) boys had slower heart rates compared to LGE(−) boys. The lower heart rates in LGE(+) boys are explained by slightly older age and increased administration of beta-blockers for heart rate management at advanced stages of disease.(39) In order to minimize the effect of heart rate, this study relied on sequence parameters in recommended guidelines.(22) In particular, the limited spatial resolution attributed to the breath-held sequence, made it challenging to completely isolate the thin wall of the RV from the blood pool. Indeed, both pre- and post-contrast T1 mapping in the RV may be biased by partial volume effects, which have been suspected of confounding T1 mapping results in the thin LV wall of patients with dilated cardiomyopathy.(10, 40) However, inclusion of RVM as a covariate in the model increased the significance of the difference between controls and LGE(–) boys as well as controls and LGE(+) boys. Partial volume effects may account for

some of this effect, but were not found to be the main driver, especially noting that the T1 values of blood were not different between the groups. The thin RV wall may also confound registration of pre- and post-contrast images necessary for estimation of ECV. Higher spatial resolution, using for example respiratory gated sequences,(41) an acquisition in systole,(30) and more slices are likely to further increase the accuracy of RV-T1 measurements.

Conclusion

Pre-contrast RV-T1 is elevated in boys with DMD compared to healthy controls and is negatively correlated with RV ejection fraction.

Supplementary Material

Refer to Web version on PubMed Central for supplementary material.

Acknowledgments

The authors of this manuscript thank all families for participating, all study coordinators and MRI technicians for their help in organizing and executing the studies, and Jarrett Rosenberg for his support with the statistical analysis.

Grant support

This study was supported by NIH R01 HL131975 to DBE, the Swiss National Research Foundation P2EZP2_188964 to SAD, and NSF DGE 1650604 to NGM.

References

1. D'Amario D, Amodeo A, Adorisio R, et al. : A current approach to heart failure in Duchenne muscular dystrophy. Heart 2017; 103:1770–1779. [PubMed: 28668906]
2. Ryder S, Leadley RM, Armstrong N, et al. : The burden, epidemiology, costs and treatment for Duchenne muscular dystrophy: An evidence review. Orphanet J Rare Dis 2017.
3. Fayssoil A, Abasse S, Silverston K: Cardiac Involvement Classification and Therapeutic Management in Patients with Duchenne Muscular Dystrophy. J Neuromuscul Dis 2017; 4:17–23. [PubMed: 28269790]
4. Meyers TA, Townsend D: Early right ventricular fibrosis and reduction in biventricular cardiac reserve in the dystrophin-deficient mdx heart. Am J Physiol - Hear Circ Physiol 2015; 308:H303–H315.
5. Larcher T, Lafoux A, Tesson L, et al. : Characterization of dystrophin deficient rats: A new model for duchenne muscular dystrophy. PLoS One 2014; 9.
6. Mavrogeni S: Cardiac involvement in Duchenne and Becker muscular dystrophy. World J Cardiol 2015; 7:410. [PubMed: 26225202]
7. McNally EM, Kaltman JR, Woodrow Benson D, et al. : Contemporary cardiac issues in Duchenne muscular dystrophy. Circulation 2015; 131:1590–1598. [PubMed: 25940966]
8. Frankel KA, Rosser RJ: The pathology of the heart in progressive muscular dystrophy: Epimyocardial fibrosis. Hum Pathol 1976; 7:375–386. [PubMed: 939536]
9. Hor KN, Taylor MD, Al-Khalidi HR, et al. : Prevalence and distribution of late gadolinium enhancement in a large population of patients with Duchenne muscular dystrophy: Effect of age and left ventricular systolic function. J Cardiovasc Magn Reson 2013; 15:107. [PubMed: 24359596]
10. Dass S, Suttie JJ, Piechnik SK, et al. : Myocardial tissue characterization using magnetic resonance noncontrast t1 mapping in hypertrophic and dilated cardiomyopathy. Circ Cardiovasc Imaging 2012; 5:726–33. [PubMed: 23071146]

11. Olivieri LJ, Kellman P, McCarter RJ, Cross RR, Hansen MS, Spurney CF: Native T1 values identify myocardial changes and stratify disease severity in patients with Duchenne muscular dystrophy. J Cardiovasc Magn Reson 2017; 18:72.
12. Riesenkampff E, Messroghli DR, Redington AN, Grosse-Wortmann L: Myocardial T1 Mapping in Pediatric and Congenital Heart Disease. Circ Cardiovasc Imaging 2015; 8.
13. Maforo NG, Magrath P, Moulin K, et al. : T1-Mapping and extracellular volume estimates in pediatric subjects with Duchenne muscular dystrophy and healthy controls at 3T. J Cardiovasc Magn Reson 2020; 22:1–13. [PubMed: 31898543]
14. Moon JC, Messroghli DR, Kellman P, et al. : Myocardial T1 mapping and extracellular volume quantification: a Society for Cardiovascular Magnetic Resonance (SCMR) and CMR Working Group of the European Society of Cardiology consensus statement. J Cardiovasc Magn Reson 2013; 15:92. [PubMed: 24124732]
15. Jerosch-Herold M, Kwong RY: Cardiac T1 imaging. Top Magn Reson Imaging 2014; 23:3–11. [PubMed: 24509619]
16. Mehmood M, Hor KN, Al-Khalidi HR, et al. : Comparison of right and left ventricular function and size in Duchenne muscular dystrophy. Eur J Radiol 2015; 84:1938–1942. [PubMed: 26210092]
17. Kellman P, Chefd'hotel C, Lorenz CH, Mancini C, Arai AE, McVeigh ER: High spatial and temporal resolution cardiac cine MRI from retrospective reconstruction of data acquired in real time using motion correction and resorting. Magn Reson Med 2009; 62:1557–1564. [PubMed: 19780155]
18. Messroghli DR, Radjenovic A, Kozerke S, Higgins D, Sivananthan M, Ridgway J: Modified Look-Locker inversion recovery (MOLLI) for high-resolution T1 mapping of the heart. Magn Reson Med 2004; 52.
19. Kellman P, Larson AC, Hsu LY, et al. : Motion-corrected free-breathing delayed enhancement imaging of myocardial infarction. Magn Reson Med 2005; 53:194–200. [PubMed: 15690519]
20. Kawel-Boehm N, Maceira A, Valsangiacomo-Buechel ER, et al. : Normal values for cardiovascular magnetic resonance in adults and children. J Cardiovasc Magn Reson 2015; 17:1–33. [PubMed: 25589308]
21. Naik SL, Rodriguez JJ, Kalra N, Sorrell VL: Tricuspid annular plane systolic excursion (TAPSE) revisited using CMR. J Cardiovasc Magn Reson 2012; 14.
22. Messroghli DR, Moon JC, Ferreira VM, et al. : Clinical recommendations for cardiovascular magnetic resonance mapping of T1, T2, T2* and extracellular volume: A consensus statement by the Society for Cardiovascular Magnetic Resonance (SCMR) endorsed by the European Association for Cardiovascular Imagi. J Cardiovasc Magn Reson 2017; 19:75. [PubMed: 28992817]
23. Chow K, Flewitt JA, Green JD, Pagano JJ, Friedrich MG, Thompson RB: Saturation recovery single-shot acquisition (SASHA) for myocardial T 1 mapping. Magn Reson Med 2014; 71:2082–2095. [PubMed: 23881866]
24. Bland JM, Altman DG: Measuring agreement in method comparison studies. Stat Methods Med Res 1999; 8:135–160. [PubMed: 10501650]
25. Plymen CM, Sado DM, Taylor AM, et al. : Diffuse myocardial fibrosis in the systemic right ventricle of patients late after Mustard or Senning surgery: an equilibrium contrast cardiovascular magnetic resonance study. Eur Hear J - Cardiovasc Imaging 2013; 14:963–968.
26. Kozak MF, Redington A, Yoo S-J, Seed M, Greiser A, Grosse-Wortmann L: Diffuse myocardial fibrosis following tetralogy of Fallot repair: a T1 mapping cardiac magnetic resonance study. Pediatr Radiol 2014; 44:403–409.
27. Karur GR, Robison S, Iwanochko RM, et al. : Use of Myocardial T1 Mapping at 3.0 T to Differentiate Anderson-Fabry Disease from Hypertrophic Cardiomyopathy. Radiology 2018; 288:398–406. [PubMed: 29688154]
28. Pagano JJ, Chow K, Khan A, et al. : Reduced Right Ventricular Native Myocardial T1 in Anderson-Fabry Disease: Comparison to Pulmonary Hypertension and Healthy Controls. PLoS One 2016; 11:e0157565. [PubMed: 27305064]

29. Freed BH, Semaan E, Benefield BC, et al. : Right Ventricular T1 Mapping: A Feasibility Study. J Hear Lung Transplant 2016; 35:S275–S276.
30. Kawel-Boehm N, Dellas Buser T, Greiser A, Bieri O, Bremerich J, Santini F: In-vivo assessment of normal T1 values of the right-ventricular myocardium by cardiac MRI. Int J Cardiovasc Imaging 2014; 30:323–328. [PubMed: 24221905]
31. García-Álvarez A, García-Lunar I, Pereda D, et al. : Association of Myocardial T1-Mapping CMR With Hemodynamics and RV Performance in Pulmonary Hypertension. JACC Cardiovasc Imaging 2015; 8:76–82. [PubMed: 25592698]
32. Freed BH, Collins JD, François CJ, et al.: MR and CT Imaging for the Evaluation of Pulmonary Hypertension. 2016.
33. Granitz M, Motloch LJ, Granitz C, et al. : Comparison of native myocardial T1 and T2 mapping at 1.5T and 3T in healthy volunteers: Reference values and clinical implications. Wien Klin Wochenschr 2019; 131:143–155. [PubMed: 30519737]
34. Mavrogeni S, Papavasiliou A, Giannakopoulou K, et al. : Oedema-fibrosis in Duchenne Muscular Dystrophy: Role of cardiovascular magnetic resonance imaging. Eur J Clin Invest 2017; 47:e12843.
35. Florian A, Ludwig A, Rösch S, Yildiz H, Sechtem U, Yilmaz A: Myocardial fibrosis imaging based on T1-mapping and extracellular volume fraction (ECV) measurement inmuscular dystrophy patients: Diagnostic value compared with conventional late gadolinium enhancement (LGE) imaging. Eur Heart J Cardiovasc Imaging 2014; 15:1004–1012. [PubMed: 24686257]
36. Hayes EA, Nandi D: Is there a future for the use of left ventricular assist devices in Duchenne muscular dystrophy? Pediatr Pulmonol 2020:ppul.25181.
37. Iodice F, Testa G, Averardi M, Brancaccio G, Amodeo A, Cogo P: Implantation of a left ventricular assist device as a destination therapy in Duchenne muscular dystrophy patients with end stage cardiac failure: Management and lessons learned. Neuromuscul Disord 2015; 25:19–23. [PubMed: 25444433]
38. Kirklin JK, Xie R, Cowger J, et al. : Second annual report from the ISHLT Mechanically Assisted Circulatory Support Registry. J Hear Lung Transplant 2018; 37:685–691.
39. Thomas TO, Morgan TM, Burnette WB, Markham LW: Correlation of heart rate and cardiac dysfunction in duchenne muscular dystrophy. Pediatr Cardiol 2012; 33:1175–1179. [PubMed: 22434508]
40. Puntmann VO, Voigt T, Chen Z, et al. : Native T1 Mapping in Differentiation of Normal Myocardium From Diffuse Disease in Hypertrophic and Dilated Cardiomyopathy. JACC Cardiovasc Imaging 2013; 6:475–484. [PubMed: 23498674]
41. Guo R, Cai X, Kucukseymen S, et al. : Free-breathing whole-heart multi-slice myocardial T 1 mapping in 2 minutes. Magn Reson Med 2020:mrm.28402.

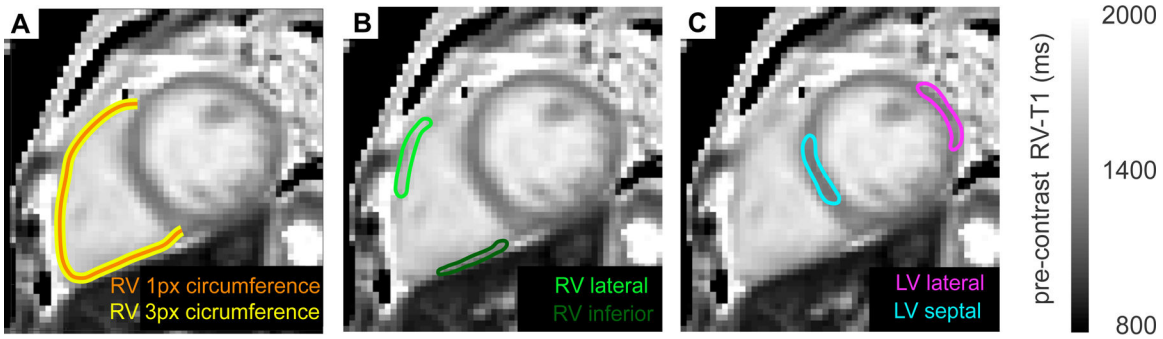

Figure 1:

Regions of interest were selected in the grey-scale images of the mid-ventricular short-axis T1 maps in the left and right ventricle (LV, RV). Four regions of interest were used in the RV (A, B) to assess the most reliable method for T1 measurement. Additionally, we measured T1 in the septum and in a segment of the lateral LV wall as intra-subject reference.

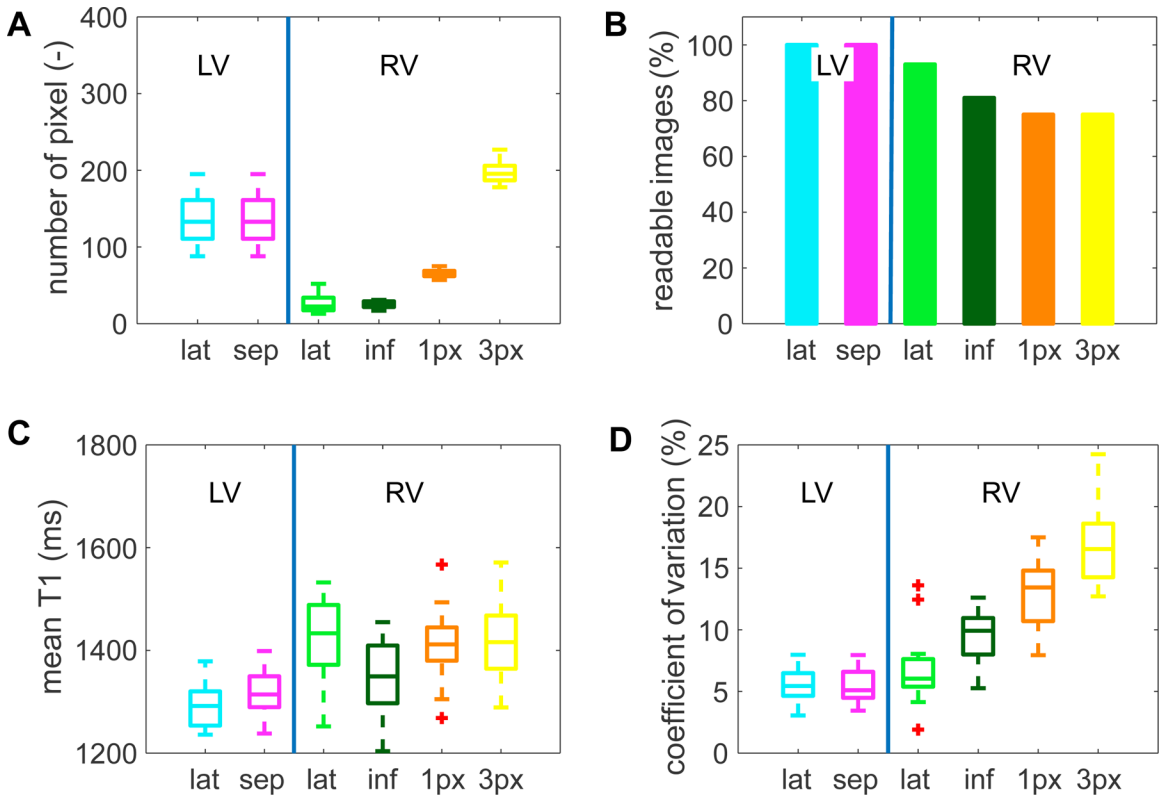

Figure 2:

Reliability of regions of interest in assessing pre-contrast T1 in the control cohort of healthy boys (N=17). The reliability was assessed as the number of pixels (A), percentage of readable images (B), mean T1 (C) and coefficient of variation inside each region of interest (ROI) (D). We report the LV and the septum as well as four ROIs in the right ventricle (RV). Lat: lateral, sep: septal, inf: inferior, 1px: 1 pixel thick circumference, 3px: 3 pixel dilated circumference.

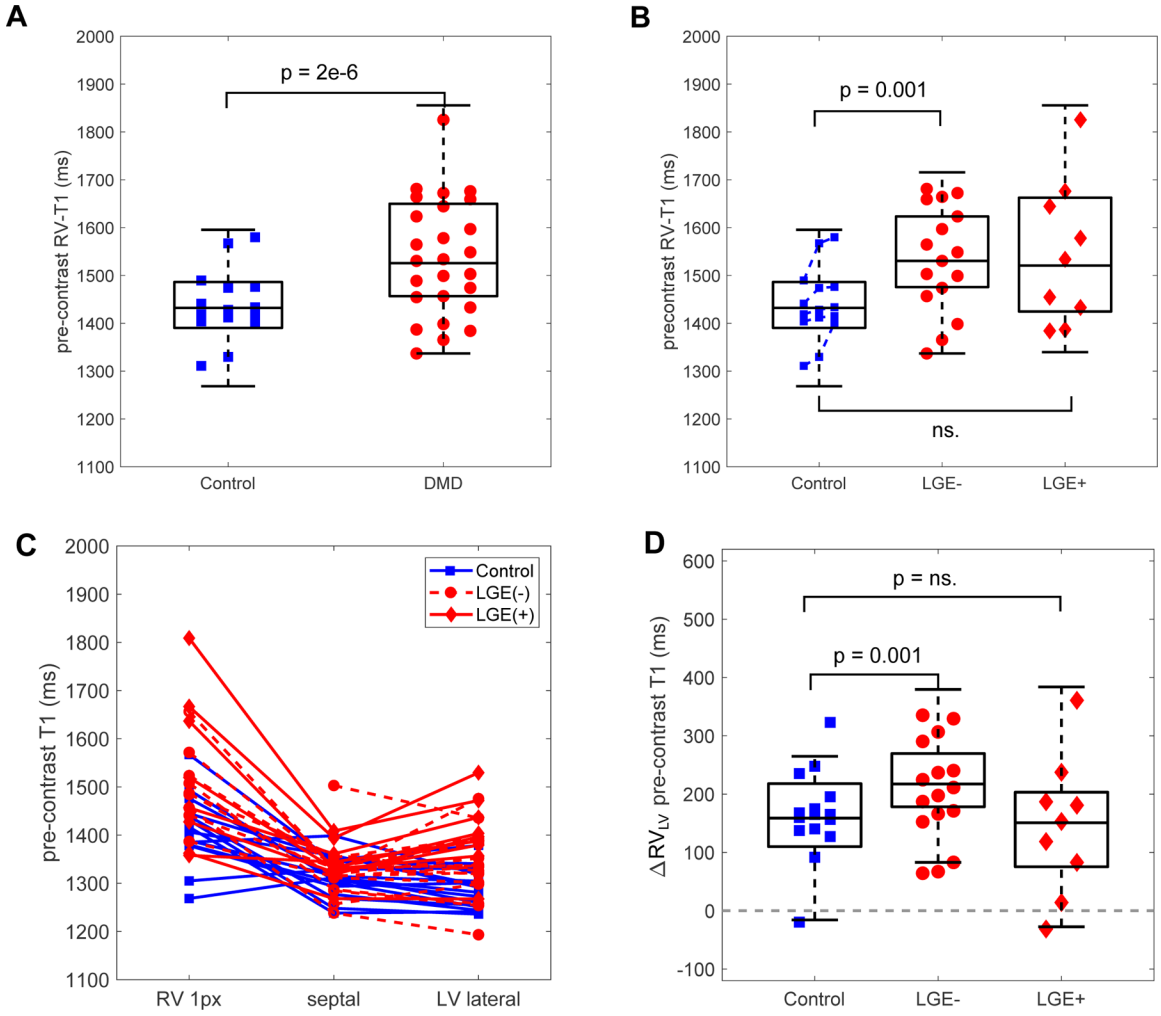

Figure 3:

Group-wise comparison of pre-contrast RV-T1. (A) DMD has significantly elevated circumferential pre-contrast RV-T1. (B) Significant differences in circumferential pre-contrast RV-T1 were found between DMD boys with negative LGE (LGE(–)) and healthy controls. (C) Values of pre-contrast T1 are similar across all segments of the heart, while they diverge for LGE(–) boys and even more for LGE(+) boys. (D) Relative RV_{LV}-T1 distinguishes controls from LGE(–) boys.

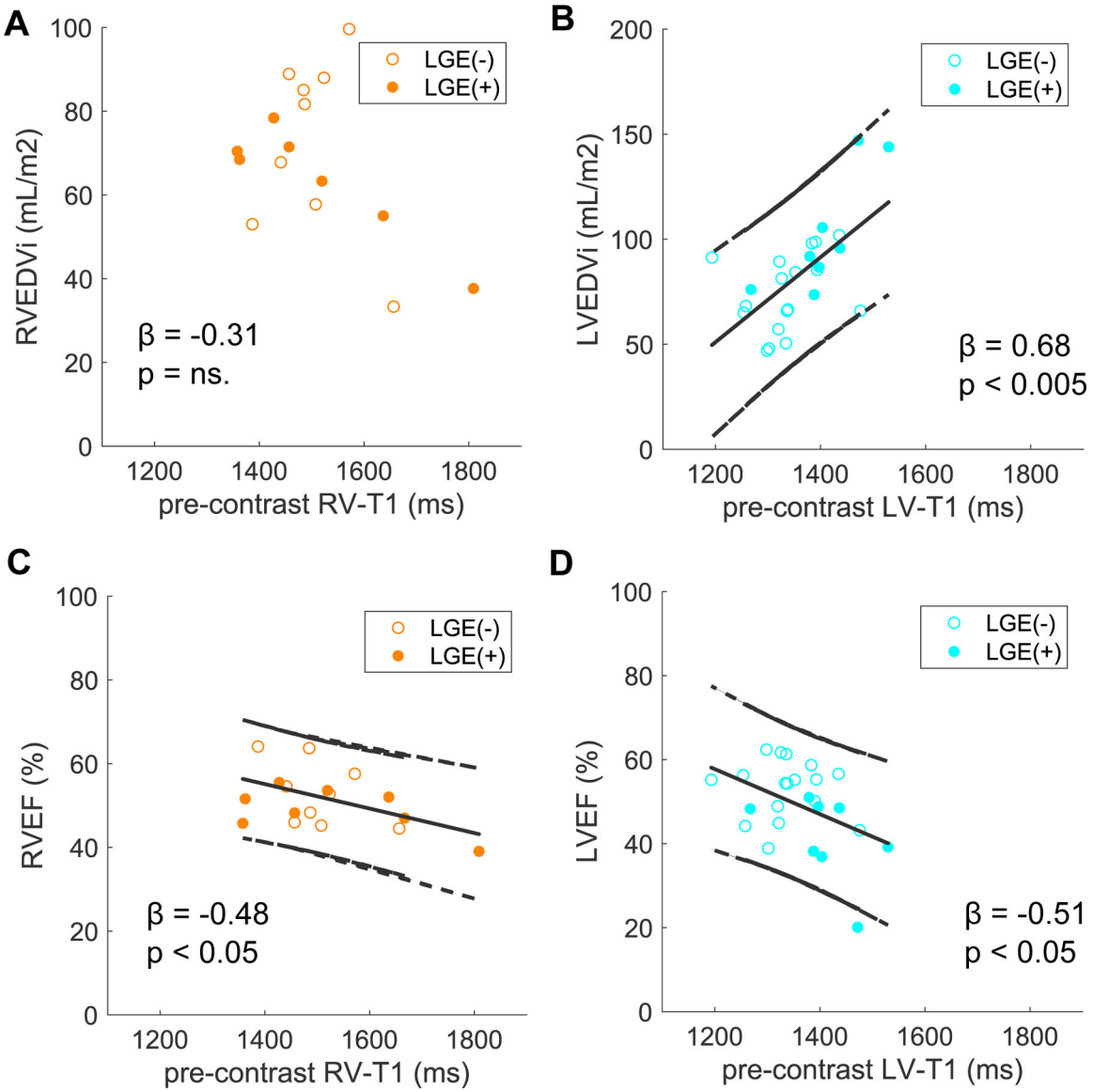

Figure 4:

An association between pre-contrast T1 and function was found in the LV for both end-diastolic volume index and ejection fraction and in the RV for ejection fraction only.

LGE: Late gadolinium enhancement, LVEDVi: Left ventricular end-diastolic volume index, RVEDVi: Right ventricular end-diastolic volume index, LVEF: Left ventricular ejection fraction (%), RVEF: right ventricular ejection fraction (%).

Table 1:

Imaging Parameters Used For Different MR Sequences

Specification	Function free-breathing	Function breath-held	Pre-contrast T1	LGE	Post-contrast T1
Sequence used	Retrospectively binned bSSFP cine	bSSFP cine	MOLLI 5(3)3, non-selective inversion pulse, SSFP	MOCO PSIR	MOLLI 4(1)3(1)2 non-selective inversion pulse, SSFP
Free-breathing	Yes	No	Yes	Yes	Yes
Flip angle (°)	40	58	20	20	20
Specifications	6/8 Fourier and rate-4 parallel imaging	rate-3 parallel imaging	7/8 partial Fourier and rate-2 parallel imaging	Rate-2 parallel imaging	7/8 partial Fourier and rate-2 parallel imaging
Matrix size (pixel)	192 × 144	256 × 192	192 × 132	192 × 120	192 × 164
Pixel size (mm)	1.9 × 1.9	1.6 × 1.6	1.9 × 1.9	1.4 × 1.4	1.9 × 1.9
Field of view (cm)	36.5 × 27.4	41.0 × 30.7	36.5 × 25.1	26.9 × 16.8	36.5 × 31.2
Slice thickness	8	6	8	6	8
Bandwidth (Hz/pixel)	930	977	1085	977	1085
Echo time (ms)	1.2	1.4	1.01	2.01	1.01
Repetition time (ms)	2.4	3.3	2.44	2.83	2.44
Temporal resolution (ms)	64.4	32.5	Single shot at diastasis	35.1	Single shot at diastasis

bSSFP: balanced steady-state free precession, MOLLI: Modified Look-Look inversion recovery, MOCO: motion-corrected, PSIR: phase-sensitive inversion recovery

Table 2:

Study Population

	Control	DMD	
		LGE(–)	LGE(+)
n	**17**	**18**	**9**
Demographics			
Age (years)	13.0(4)	12.5(3)	15.0(6.5)
Height (m)	1.65(0.2) †	1.34(0.28)	1.4(0.28)
Weight (kg)	51.3(15)	46.9(31)	50(15)
BMI (kg/m^2)	18.2(3.3) †	23.6(1.2)	25.6(2.6)
BSA (m^2)	1.53(0.32) †	1.39(0.37)	1.34(0.48)
HR (bpm)	68.6(30) †	93(25) *	77.4(16)
Hematocrit (%)	-	43.8(4.6)	43.4(2.7)
Race			
Caucasian	13	11	5
African American	0	1	0
Asian	1	2	2
Other	2	1	2
Mixed	1	3	0
Ethnicity			
Hispanic/Latino	6	6	4
Medication			
ACEi	0	14(78%)	6(67%)
ARB	0	2(11%)	2(22%)
β-blocker	0	4(22%)	3(33%)
Corticosteroids	0	11(61%)	7(78%)
Diuretics	0	9(50%)	7(78%)
Functional metrics			
LVEDVi (mL/m^2)	86.2(18)	74.8(24) *	93.8(43)
LVESVi (mL/m^2)	37.2(8.9)	36.9(11) **	47.4(32)
LVEF (%)	57.8(5.8) ††	55.2(9.8) **	43.8(11)
LVMi (g/m^2)	38.1(8.1)	32.7(8)	38.8(11)
LVM/LVEDV (g/mL)	0.452(0.11)	0.469(0.17)	0.409(0.13)
RVEDVi (mL/m^2)	89.1(22) ††	73.6(33)	70.5(16)
RVESVi (mL/m^2)	39.3(7.5) †	31.8(19)	34.8(10)
RVEF (%)	54.2(7.2)	53.6(12)	48.2(5.7)
RVMi (g/m^2)	29.8(7.2) ††	24.7(6.4)	21.7(5.4)

	Control	DMD	
		LGE(–)	LGE(+)
n	**17**	**18**	**9**
RVM/RVEDV (g/mL)	0.328(0.04)	0.338(0.05)	0.337(0.08)
TAE (mm)	26.0(5)††	22.2(3)	22.0(4)

Data is reported as median (interquartile range). BMI: Body mass index, BSA: Body surface area, HR: Heart rate, Left ventricular (LV), Right ventricular (RV), End-diastolic volume index (EDVi), End-systolic volume index (ESVi), Ejection fraction (EF), Mass (M), TAE: Tricuspid annular excursion.

*: p<0.05 between LGE(+)/LGE(–);

**: p<0.005 between LGE(+)/LGE(–);

†: p<0.05 between control and all boys with DMD;

††: p<0.005 between control and all boys with DMD

Table 3:

Intra-scan and intra-observer agreement of pre-contrast T1 in boys with DMD.

Bland-Altman		**N**	**ICC**	**Mean Δ**	**SD Δ**	**95% LOA**
Scan-1 vs. Scan-2	RV lateral	23	0.76	43.3	82.0	(–117.30 – 203.98)
	RV inferior	21	0.83	64.3	45.6	(–25.11 – 153.64)
	RV 1px	15	0.96	20.6	30.0	(–37.41 – 78.68)
	RV 3px	15	0.97	22.1	27.5	(–31.75 – 75.98)
O1a vs. O1b	RV lateral	22	0.63	20.1	110.7	(–196.95 – 237.09)
	RV inferior	22	0.86	11.1	57.7	(–124.05 – 101.95)
	RV 1px	14	0.92	14.9	50.7	(–84.56 – 114.33)
	RV 3px	14	0.79	20.8	84.0	(–185.50 – 143.84)
Mixed-effect model		**N**	**ICC**			**95% CI**
All readers (O1, O2, O3)	RV lateral	49	0.60	-	-	[0.38 – 0.79]
	RV inferior	46	0.78	-	-	[0.62 – 0.88]
	RV 1px	37	0.94	-	-	[0.88 – 0.97]
	RV 3px	37	0.89	-	-	[0.79 – 0.94]

S: Scan, O: Observer, RV: right ventricle, ICC: Intra-class correlation, SD: Standard deviation, LOA: Limits of agreement, CI: Confidence interval

Table 4:

Pre-contrast T1 comparison between boys with DMD and healthy controls.

	Control	DMD	
		LGE(–)	LGE(+)
n	**17**	**18**	**9**
RV 1px T1 (ms)	1436 [1399 – 1473]	1543 [1489 – 1597] **	1550 [1402 – 1699] †
RV inferior T1 (ms)	1345 [1306 – 1385]	1388 [1321 – 1455]	1483 [1288 – 1679] ††
LV lateral T1 (ms)	1290 [1269 – 1311]	1335 [1297 – 1373] *	1409 [1346 – 1473] **
Septal T1 (ms)	1316 [1294–1337]	1326 [1295–1357]	1344[1306 – 1381]
ΔRVSep T1 (ms)	149 [109 – 190]	206 [155 – 257] ††	141 [33 – 249]
ΔRVLV T1 (ms)	122 [78 – 166]	219 [167 – 270] **,†	205 [85 – 325] ††
ΔLVSep T1 (ms)	–25.5 [−41.0 – −10.0]	9.1 [−18.6 – 36.8] *	65.8 [33.9 – 97.6] **

Data is reported as mean [confidence interval]. Univariate comparison using a Wilcoxon rank sum test comparing LGE(–)/LGE(+) against control group:

* p<0.05

** p<0.005. Multivariate prediction for LGE(–)/LGE(+) from control group with right ventricular mass and body mass index as covariates (only for RV):

† p<0.05,

†† p<0.005. Left ventricular: LV, Right ventricular: RV